

h*-BOX METHODS FOR THE APPROXIMATION OF HYPERBOLIC CONSERVATION LAWS ON IRREGULAR GRIDS

MARSHA J. BERGER[†], CHRISTIANE HELZEL[†], AND RANDALL J. LEVEQUE[‡]

Abstract. We study generalizations of the high-resolution wave propagation algorithm for the approximation of hyperbolic conservation laws on irregular grids that have a time step restriction based on a reference grid cell length that can be orders of magnitude larger than the smallest grid cell arising in the discretization. This Godunov-type scheme calculates fluxes at cell interfaces by solving Riemann problems defined over boxes of a reference grid cell length h .

We discuss stability and accuracy of the resulting so-called h -box methods for one-dimensional systems of conservation laws. An extension of the method for the two-dimensional case, which is based on the multidimensional wave propagation algorithm, is also described.

Key words. finite volume methods, conservation laws, nonuniform grids, stability, accuracy

AMS subject classifications. 35L65, 65M12

PII. S0036142902405394

1. Introduction. We consider the numerical approximation of hyperbolic systems of conservation laws using finite volume schemes on irregular grids. We mainly restrict our considerations to the case of one spatial dimension, although an extension to the two-dimensional case will also be considered. Under appropriate smoothness assumptions the equations can be formulated in the differential form

$$(1.1) \quad \frac{\partial}{\partial t} q(x, t) + \frac{\partial}{\partial x} f(q(x, t)) = 0,$$

where $q(x, t)$ is a vector of conserved quantities and $f(q(x, t))$ is a vector of flux functions. For the numerical approximation we want to use a finite volume method. On an unstructured grid such a scheme can be written in the general form

$$(1.2) \quad Q_i^{n+1} = Q_i^n - \frac{\Delta t}{\Delta x_i} \left(F_{i+\frac{1}{2}} - F_{i-\frac{1}{2}} \right),$$

where Q_i^n is an approximation of the cell average of the conserved quantity over the grid cell $[x_{i-\frac{1}{2}}, x_{i+\frac{1}{2}}]$ at time $t = t^n$. The vector valued quantities $F_{i-\frac{1}{2}}$ and $F_{i+\frac{1}{2}}$ are the numerical flux functions at the cell interfaces. We denote the time step by Δt and the length of the i th grid cell by $\Delta x_i = x_{i+\frac{1}{2}} - x_{i-\frac{1}{2}}$.

We are particularly interested in the construction of high-resolution schemes for a grid which contains one small grid cell, while all other grid cells have the same length, which will be denoted by $h = \Delta x$. This situation is motivated by a two-dimensional application, namely the construction of Cartesian grid methods with embedded irregular geometry. Away from the boundary one may want to use a

*Received by the editors April 10, 2002; accepted for publication (in revised form) November 1, 2002; published electronically May 22, 2003.

<http://www.siam.org/journals/sinum/41-3/40539.html>

[†]Courant Institute of Mathematical Sciences, 251 Mercer Street, New York, NY 10012-1185 (berger@cims.nyu.edu, helzel@cims.nyu.edu). The work of these authors was supported by DOE grants DE-FG02-88ER25053 and DE-FC02-01ER25472, and AFOSR grant F49620-00-1-0099.

[‡]Department of Applied Mathematics, University of Washington, Box 352420, Seattle, WA 98195-2420 (rjl@amath.washington.edu). The work of this author was supported by DOE grants DE-FG03-00ER25292 and DE-FC02-01ER25474, and NSF grant DMS-0106511.

regular Cartesian grid. Near the boundary one then obtains irregular cut cells, which may be orders of magnitude smaller than the regular grid cells. Our aim in such a situation is to construct a scheme that is stable based on time steps adequate for the regular grid. Such methods were developed by Berger and LeVeque in [4], [5], [6]. The basic idea of these so-called h -box methods is to approximate the numerical fluxes at the interfaces of a small cell based on initial values specified over regions of length h , i.e., of the length of a regular grid cell. If this is done in an appropriate way, then the resulting method remains stable for time steps based on a CFL number appropriate for the regular part of the grid. See also [8], [9], [10], [23], [21], and [25] for other embedded boundary Cartesian grid methods that have this same stability property.

Besides this two-dimensional application, h -box schemes can also offer interesting alternatives to existing irregular grid methods. An extension of h -box methods to a completely irregular grid was considered by Berger, LeVeque, and Stern [7]; see also Stern [28]. We will consider such calculations in section 5. In section 7, we construct a multidimensional h -box method. Other potential applications are the construction of moving mesh or front-tracking algorithms. Stern [28] used an h -box method to construct a conservative finite volume algorithm for a Cartesian grid with an embedded curvilinear grid.

Unsurprisingly, the accuracy of an h -box method depends strongly on the definition of the h -box values. In this paper we develop a one-dimensional as well as a two-dimensional high-resolution h -box method. Our goal here is a systematic study of h -box methods in a relatively simple context to provide fundamental understanding for the more complex applications mentioned above. For the advection equation we show that the one-dimensional scheme leads to a second order accurate approximation of smooth solutions on nonuniform grids (without any restrictions on the grid). We also verify that the resulting method leads to high-resolution approximations for the Euler equations on nonuniform meshes. The approximation of transonic rarefaction waves turns out to require a special treatment. Throughout this paper we will discuss the construction of h -box methods based on LeVeque's high-resolution wave propagation algorithm [18]. This method is implemented in the CLAWPACK software package [13], which provided the basic tool for our test calculations.

The large time step Godunov method of LeVeque described in [14], [15], [16] is related to the h -box method. This scheme allows larger time steps in the approximation of nonlinear systems of conservation laws by increasing the domain of influence of the numerical scheme. This is done in a wave propagation approach, in which waves are allowed to move through more than one mesh cell. The interaction of waves is approximated by linear superposition. At a reflecting boundary this method becomes more difficult than an h -box method, especially in higher dimensions, since the reflection of waves at the boundary has to be considered for waves generated by Riemann problems away from the boundary; see [3]. In [22, Lemma 3.5], Morton showed that high-resolution versions of such a large time step method lead to a second order accurate approximation of the one-dimensional advection equation on a nonuniform grid only if the grid varies smoothly. The high-resolution h -box method described in this paper does not require this smoothness assumption.

2. The wave propagation algorithm. In this section we describe the basic concept of the high-resolution wave propagation algorithm applied to irregular Cartesian grids; a more general description can be found in LeVeque [18] or [19]. The numerical method for solving (1.1) is a Godunov-type method; i.e., the fluxes at cell interfaces are calculated by solving Riemann problems defined from cell averages of

the conserved quantities. This is done by calculating waves that are moving into each grid cell. The first order update of the wave propagation algorithm has the form

$$Q_i^{n+1} = Q_i^n - \frac{\Delta t}{\Delta x_i} \left(\mathcal{A}^+ \Delta Q_{i-\frac{1}{2}} + \mathcal{A}^- \Delta Q_{i+\frac{1}{2}} \right).$$

Here the change of the conserved quantities is calculated by taking all waves into account that are moving into the grid cell from the left (respectively, right) cell interface. The solution of Riemann problems at cell interfaces provides a decomposition of the jump $Q_{i+1}^n - Q_i^n$ into waves $\mathcal{W}_{i+\frac{1}{2}}^p$ that are moving with speed $s_{i+\frac{1}{2}}^p$ for $1 \leq p \leq M_w$,

$$\Delta Q_{i+\frac{1}{2}}^n = Q_{i+1}^n - Q_i^n = \sum_{p=1}^{M_w} \mathcal{W}_{i+\frac{1}{2}}^p.$$

The left- and right-going fluctuations are calculated as

$$\mathcal{A}^+ \Delta Q_{i-\frac{1}{2}} = \sum_{p=1}^{M_w} \max(s_{i-\frac{1}{2}}^p, 0) \mathcal{W}_{i-\frac{1}{2}}^p, \quad \mathcal{A}^- \Delta Q_{i+\frac{1}{2}} = \sum_{p=1}^{M_w} \min(s_{i+\frac{1}{2}}^p, 0) \mathcal{W}_{i+\frac{1}{2}}^p.$$

This can be written as a finite volume scheme of the form (1.2) using the relations

$$(2.1) \quad F_{i+\frac{1}{2}} = f(Q_i) + \mathcal{A}^- \Delta Q_{i+\frac{1}{2}},$$

$$(2.2) \quad F_{i-\frac{1}{2}} = f(Q_i) - \mathcal{A}^+ \Delta Q_{i-\frac{1}{2}}.$$

Appropriate waves and speeds for systems of conservation laws can sometimes be calculated by using an exact Riemann solver, but more often an approximative Riemann solver, for instance a Roe–Riemann solver [26], is used.

In the wave propagation algorithm second order correction terms are included by extending the first order method into the form

$$(2.3) \quad Q_i^{n+1} = Q_i^n - \frac{\Delta t}{\Delta x_i} \left(\mathcal{A}^+ \Delta Q_{i-\frac{1}{2}} + \mathcal{A}^- \Delta Q_{i+\frac{1}{2}} \right) - \frac{\Delta t}{\Delta x_i} \left(\tilde{F}_{i+\frac{1}{2}}^2 - \tilde{F}_{i-\frac{1}{2}}^2 \right).$$

On an irregular grid, the second order correction terms have the form

$$(2.4) \quad \tilde{F}_{i+\frac{1}{2}}^2 = \frac{1}{2} \sum_{p=1}^{M_w} |s_{i+\frac{1}{2}}^p| \left(\frac{\Delta x_i}{(\Delta x_i + \Delta x_{i+1})/2} - \frac{\Delta t}{(\Delta x_i + \Delta x_{i+1})/2} |s_{i+\frac{1}{2}}^p| \right) \tilde{\mathcal{W}}_{i+\frac{1}{2}}^p.$$

In (2.4) the waves $\tilde{\mathcal{W}}^p$ are limited waves—this limiting is necessary in order to avoid oscillations near discontinuities.

The resulting scheme is stable for the approximation of systems of conservation laws (1.1) as long as time steps are restricted such that waves move through at most one mesh cell, which means the Courant number is no larger than one, i.e.,

$$(2.5) \quad \text{CFL} = \Delta t \max_i \left(\frac{\max(\max_p(s_{i-\frac{1}{2}}^p, 0), |\min_p(s_{i+\frac{1}{2}}^p, 0)|)}{\Delta x_i} \right) \leq 1.$$

The *h*-box method changes this time step restriction by replacing Δx_i in the denominator of (2.5) by *h*, the width of a reference grid cell. We will use the notation CFL_h if we want to indicate that the Courant number is based on grid cells of width *h*.

We want to note that some care is necessary in the construction of second order accurate algorithms for irregular grids. There exist versions of the one-dimensional Lax–Wendroff method which lead to second order accurate approximations of the advection equation only if the grid is sufficiently smooth, i.e., if $\Delta x_i/\Delta x_{i-1} = 1 + \mathcal{O}(h)$, where $h = \max_i \Delta x_i$; see, for instance, Wendroff and White [30], [31] and Pike [24]. See also Morton [22] for convergence results of finite volume methods for the approximation of the advection equation on nonuniform grids.

3. The one-dimensional h -box method. First we want to approximate (1.1) on an almost uniform grid that contains one small grid cell in the middle. This example allows simple analytical studies. However, we will show that the results obtained for this simple test case can be extended to more general applications.

We denote the length of a regular grid cell by $h = \Delta x$. The small cell has the length αh , with $0 < \alpha \leq 1$. For the small cell the numerical method has to be modified in order to obtain a stable scheme for time steps Δt that satisfy the stability condition in the regular part of the grid. The h -box method introduced by Berger and LeVeque [5] defines new left and right states at the edges of the small cell that represent the conserved quantities at these interfaces over boxes of length h ; see Figure 1. This guarantees that the domain of dependence of the numerical solution has the size of a regular mesh cell, which is a necessary stability condition.

3.1. First order accurate h -box methods. As a first step we compare the performance of two different h -box schemes applied to the advection equation $q_t(x, t) + aq_x(x, t) = 0$. We will assume that $a > 0$, although analogous considerations can of course be made for the case $a < 0$. In the following we assume that k is the index of the small cell. In order to calculate numerical fluxes at the small cell interfaces new values of the conserved quantity q that represent piecewise constant initial values over boxes of length h will be defined. For the left cell interface of the small cell, these values are denoted by $Q_{k-\frac{1}{2}}^L$ and $Q_{k-\frac{1}{2}}^R$. At the right cell interface of the small cell we have to define values $Q_{k+\frac{1}{2}}^L$ and $Q_{k+\frac{1}{2}}^R$. This is indicated by the shaded boxes at each interface in Figure 1.

The most obvious choice is to define the h -box values via cell averaging over the piecewise constant initial values. (To keep the notation simple we sometimes suppress the time index if it is clear that we mean the values at time t^n .) We obtain

$$(3.1) \quad \begin{aligned} Q_{k-\frac{1}{2}}^L &= Q_{k-1}, & Q_{k-\frac{1}{2}}^R &= \alpha Q_k + (1 - \alpha)Q_{k+1}, \\ Q_{k+\frac{1}{2}}^L &= \alpha Q_k + (1 - \alpha)Q_{k-1}, & Q_{k+\frac{1}{2}}^R &= Q_{k+1}. \end{aligned}$$

Such h -box values were used in Berger and LeVeque [5] as well as by Forrer and Jeltsch [10]. For the advection equation the update of the small cell value can now be calculated using the upwind method. We obtain

$$(3.2) \quad \begin{aligned} Q_k^{n+1} &= Q_k^n - \frac{\Delta t}{\alpha h} \left(aQ_{k+\frac{1}{2}}^L - aQ_{k-\frac{1}{2}}^L \right) \\ &= Q_k^n - \frac{a\Delta t}{\alpha h} \left(\alpha Q_k^n + (1 - \alpha)Q_{k-1}^n - Q_{k-1}^n \right) \\ &= Q_k^n - \frac{a\Delta t}{h} (Q_k^n - Q_{k-1}^n). \end{aligned}$$

Note that the small denominator (that may cause a stability problem) has been removed. One can indeed show TVD stability for this method assuming $\text{CFL}_h \leq 1$;

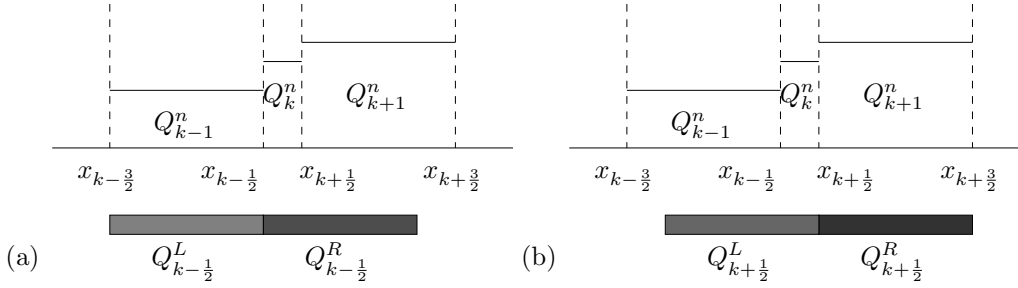


FIG. 1. Schematic description of h -box values assigned to the left small cell interface (see (a)) (respectively, the right small cell interface (see (b))).

see section 4. However, it is clear that this cannot be a very accurate formula. The truncation error of the scheme (3.2) has the form

$$\begin{aligned}
 Lq &= \frac{q_k^{n+1} - q_k^n}{\Delta t} + a \frac{q_k^n - q_{k-1}^n}{h} \\
 &= q_t(x_k, t^n) + \frac{a}{2}(\alpha + 1)q_x(x_k, t^n) + \mathcal{O}(\Delta t, h) \\
 &= \frac{a}{2}(\alpha - 1)q_x(x_k, t^n) + \mathcal{O}(\Delta t, h).
 \end{aligned}$$

Only for $\alpha = 1$ is the truncation error in cell k of the order $\mathcal{O}(\Delta t, h)$. Note that grid functions for the exact solution q are expressed with lower-case letters, whereas numerical approximations are written in capital letters.

In spite of the apparent inconsistency of the scheme, numerical tests suggest that this h -box method converges with first order. For the advection equation we can indeed prove that under appropriate smoothness assumptions the scheme is first order accurate in the small cell. This so-called *supraconvergence property* can be shown using an idea developed for conservation laws by Wendroff and White [30], [31]. See also [12], [20], where these ideas were introduced for boundary value problems for ODEs.

PROPOSITION 1. *We consider the approximation of the advection equation on an almost uniform grid with mesh width h that contains one small mesh cell of length αh , with $\alpha \leq 1$. The one-dimensional h -box method (3.2), based on an upwind discretization with h -box values calculated by averaging over piecewise constant cell average values, leads to a first order accurate approximation for sufficiently smooth solutions of the advection equation, in spite of the fact that the truncation error indicates inconsistency.*

Proof. The basic step of the proof is to calculate the local truncation error for a grid function w , which must be an accurate enough approximation of the grid function of the exact solution q . We want to show that the truncation error for w is first order, i.e., $Lw = \mathcal{O}(h)$. In order to do this we specify the grid function to have the form

$$w_i^n = q_i^n + \frac{1}{2}(1 - \alpha_i)hq_x(x_i, t^n).$$

Here we assume that $\Delta x_i = \alpha_i h$, i.e., $\alpha_i = 1$ for $i \neq k$ and $\alpha_k = \alpha$. The distance between x_k and x_{k-1} is $\frac{1}{2}h(1 + \alpha)$. In the simple situation of only one small grid cell we have $w_i^n = q_i^n$ for $i \neq k$ and $w_k^n = q_k^n + \frac{1}{2}(1 - \alpha)hq_x(x_k, t^n)$. The truncation error

of the grid function w for the scheme (3.2) has in the small cell the form

$$\begin{aligned}
 Lw &= \frac{w_k^{n+1} - w_k^n}{\Delta t} + a \frac{w_k^n - w_{k-1}^n}{h} \\
 &= \frac{q_k^{n+1} + \frac{1}{2}(1 - \alpha)hq_x(x_k, t^{n+1}) - q_k^n - \frac{1}{2}(1 - \alpha)hq_x(x_k, t^n)}{\Delta t} \\
 &\quad + a \frac{q_k^n + \frac{1}{2}(1 - \alpha)hq_x(x_k, t^n) - q_{k-1}^n}{h} + \mathcal{O}(\Delta t, h) \\
 &= \frac{q_k^n + \Delta tq_t(x_k, t^n) + \frac{1}{2}(1 - \alpha)hq_x(x_k, t^n) - q_k^n - \frac{1}{2}(1 - \alpha)hq_x(x_k, t^n)}{\Delta t} \\
 &\quad + a \frac{q_k^n + \frac{1}{2}(1 - \alpha)hq_x(x_k, t^n) - q_k^n + \frac{1}{2}(1 + \alpha)hq_x(x_k, t^n)}{h} + \mathcal{O}(\Delta t, h) \\
 &= q_t(x_k, t^n) + aq_x(x_k, t^n) + \mathcal{O}(\Delta t, h) = \mathcal{O}(\Delta t, h).
 \end{aligned}$$

From the truncation error of w and the stability of the method for $CFL_h \leq 1$ it follows that $|w_k - Q_k| = \mathcal{O}(\Delta t, h)$. Since $w = q + \mathcal{O}(h)$ we obtain the estimate

$$|q_k - Q_k| = \mathcal{O}(h);$$

i.e., the h -box method (3.2) leads to a first order accurate approximation of the advection equation in the small cell k , in spite of the fact that the scheme is inconsistent in the small cell. Using the same grid function w one can also show that the truncation error Lw in cell $k + 1$ is of the order $\mathcal{O}(h)$. In all other regularly spaced grid cells, the method agrees with the upwind scheme for which the truncation error is also $\mathcal{O}(h)$. Therefore, we obtain first order convergence in the whole domain. \square

In order to obtain a more accurate small cell scheme, we will now consider the construction of h -box values based on linear interpolation using again grid cell values that are overlapped by the h -boxes. Such h -box values have the general form

$$\begin{aligned}
 Q_{k-\frac{1}{2}}^L &= Q_{k-1}, & Q_{k-\frac{1}{2}}^R &= \lambda Q_k + (1 - \lambda)Q_{k+1}, \\
 Q_{k+\frac{1}{2}}^L &= \lambda Q_k + (1 - \lambda)Q_{k-1}, & Q_{k+\frac{1}{2}}^R &= Q_{k+1}.
 \end{aligned}$$

We want to determine λ so that we obtain a consistent h -box scheme, i.e., for which $Lq = \mathcal{O}(h, \Delta t)$. By again using Taylor series expansion we find that only $\lambda = \frac{2\alpha}{1+\alpha}$ leads to an upwind method that satisfies this condition. This suggests that the h -box values should have the form

$$\begin{aligned}
 (3.3) \quad Q_{k-\frac{1}{2}}^L &= Q_{k-1}, & Q_{k-\frac{1}{2}}^R &= \frac{2\alpha Q_k + (1 - \alpha) Q_{k+1}}{1 + \alpha}, \\
 Q_{k+\frac{1}{2}}^L &= \frac{2\alpha Q_k + (1 - \alpha) Q_{k-1}}{1 + \alpha}, & Q_{k+\frac{1}{2}}^R &= Q_{k+1}.
 \end{aligned}$$

Note that this interpolation formula was already given in [4] but not further investigated there. In [7], [28] h -box values were defined in a similar way, and the resulting scheme was shown to give good results for advection and Burgers’s equation.

One time step of the h -box method based on the interpolation formula (3.3) again for $a > 0$ has in the small cell the form

$$(3.4) \quad Q_k^{n+1} = Q_k^n - \frac{a\Delta t}{h} \cdot \frac{Q_k^n - Q_{k-1}^n}{(1 + \alpha)/2}.$$

We can derive the same method as a finite difference scheme by replacing $q_x(x_k, t^n)$ in the Taylor series expansion of

$$(3.5) \quad \begin{aligned} q(x_k, t^n + \Delta t) &= q(x_k, t^n) + \Delta t q_t(x_k, t^n) + \mathcal{O}(\Delta t^2) \\ &= q(x_k, t^n) - \Delta t \cdot a \cdot q_x(x_k, t^n) + \mathcal{O}(\Delta t^2) \end{aligned}$$

by an appropriate first order accurate finite difference formula. The *h*-box method (3.4) can be interpreted as a finite difference scheme that approximates the $q_x(x_k)$ terms by one-sided finite differences. This *h*-box method leads to a first order accurate method that approximates linear functions exactly. One can also show that an upwind scheme based on the *h*-box values (3.3) also leads to a consistent first order accurate update in the two neighboring grid cells of the small cell.

If we use the wave propagation algorithm, then the first order update in the small cell can be written in the form

$$(3.6) \quad Q_k^{n+1} = Q_k^n - \frac{\Delta t}{\alpha h} \left(\mathcal{A}^+ \Delta \hat{Q}_{k-\frac{1}{2}} - f(Q_{k-\frac{1}{2}}^R) + \mathcal{A}^- \Delta \hat{Q}_{k+\frac{1}{2}} + f(Q_{k+\frac{1}{2}}^L) \right),$$

with $\Delta \hat{Q}_{k-\frac{1}{2}} = Q_{k-\frac{1}{2}}^R - Q_{k-\frac{1}{2}}^L$ and $\Delta \hat{Q}_{k+\frac{1}{2}} = Q_{k+\frac{1}{2}}^R - Q_{k+\frac{1}{2}}^L$. In the limit case $\alpha = 1$ we have $Q_{k-\frac{1}{2}}^R = Q_{k+\frac{1}{2}}^L$, and (3.6) reduces to the first order accurate wave propagation algorithm that is valid in the regular parts of the grid. This formula remains valid for nonlinear equations as well as systems of conservation laws, assuming we have a Riemann solver that provides us a decomposition of $Q^R - Q^L$, as described in section 2. We indicate quantities that are calculated from *h*-box values by the “^” symbol.

Numerical results shown in section 5 will demonstrate the superior properties of an *h*-box method with *h*-boxes obtained by linear interpolation.

3.2. A second order accurate *h*-box method. In order to obtain a high-resolution scheme we want to include second order correction terms. This means we want to obtain an update of the small cell that can be written as

$$\begin{aligned} Q_k^{n+1} &= Q_k^n - \frac{\Delta t}{\alpha h} \left(\mathcal{A}^+ \Delta \hat{Q}_{k-\frac{1}{2}} - f(Q_{k-\frac{1}{2}}^R) + \mathcal{A}^- \Delta \hat{Q}_{k+\frac{1}{2}} + f(Q_{k+\frac{1}{2}}^L) \right) \\ &\quad - \frac{\Delta t}{\alpha h} \left(\hat{F}_{k+\frac{1}{2}}^2 - \hat{F}_{k-\frac{1}{2}}^2 \right), \end{aligned}$$

where \hat{F}^2 denotes the second order correction terms that are implemented in flux differencing form. By analogy to the standard wave propagation algorithm, these second order correction terms should also be calculated by using the waves and speeds obtained from solving Riemann problems at the cell interfaces. For the small cell we again use the waves and speeds from Riemann problems defined by the same *h*-box values used to obtain the first order update. We will restrict our consideration to *h*-box values that are calculated using the interpolation formula (3.3).

The formula (2.4) for the second order correction flux on irregular grids suggests using correction terms of the form

$$(3.7) \quad \hat{F}_{i+\frac{1}{2}}^2 = \frac{1}{2} \sum_{p=1}^{M_w} \left(\frac{1}{(1+\alpha)/2} - \frac{\Delta t}{(1+\alpha)h/2} |\hat{s}_{i+\frac{1}{2}}^p| \right) \cdot |\hat{s}_{i+\frac{1}{2}}^p| \cdot \hat{\mathcal{W}}_{i+\frac{1}{2}}^p \quad (i = k-1, k)$$

in the small cell. The waves $\hat{\mathcal{W}}_{i+\frac{1}{2}}^p$ and the speeds $\hat{s}_{i+\frac{1}{2}}^p$ can be obtained by solving Riemann problems defined by the *h*-box values at the small cell interfaces. One can

show that the truncation error in the small cell that results from such a high-resolution wave propagation scheme is $Lq_k = \mathcal{O}(h^2, \Delta t^2)$; i.e., assuming the scheme is stable we would obtain a second order accurate approximation in the small cell. However, numerical tests showed that such an approach is not stable for time steps satisfying $\text{CFL}_h \leq 1$.

Instead we use second order correction terms of the form

$$(3.8) \quad \hat{F}_{i+\frac{1}{2}}^2 = \frac{1}{2} \sum_{p=1}^{M_w} \left(1 - \frac{\Delta t}{h} |\hat{s}_{i+\frac{1}{2}}^p| \right) \cdot |\hat{s}_{i+\frac{1}{2}}^p| \hat{W}_{i+\frac{1}{2}}^p \quad (i = k - 1, k).$$

The waves are again calculated from Riemann problems defined by the h -box values. The difference from (3.7) is that we do not take the size of the small cell into account in the calculation of the correction fluxes. This reflects the general concept of the h -box method where fluxes are calculated from values defined over regions of length h .

Although the truncation error for the grid cell k now contains first order terms which do not cancel out, the numerical results are very satisfying and indicate second order convergence as well as stability for $\text{CFL}_h \leq 1$. Assuming that the solution is sufficiently smooth we can indeed prove that the resulting method leads to a second order accurate approximation for the advection equation.

PROPOSITION 2. *We consider the approximation of the advection equation on an almost uniform grid with mesh width h that contains one small mesh cell of length αh , with $\alpha \leq 1$. The h -box method consisting of the first order update (3.4) and the second order correction terms (3.8) (without limiters) leads to a second order accurate approximation for sufficiently smooth solutions of the advection equation.*

Proof. We again use the idea of Wendroff and White and consider the truncation error Lw for a grid function of the form $w_i^n = q_i^n + \frac{1}{8}h^2(\alpha_i + 1)(\alpha_i - 1)q_{xx}(x_i, t^n)$. Here we assume that $\Delta x_i = \alpha_i h$. We have $\alpha_i = 1$ for $i \neq k$ and $\alpha_k = \alpha$. In regular grid cells $i \neq k$ the grid function w agrees with the exact solution. We want to show only second order convergence in the small cell as well as in the two neighboring cells $k - 1$ and $k + 1$, since the method reduces to the high-resolution wave propagation algorithm in the other regular grid cells. In the case considered here, the wave propagation algorithm on the regular part of the grid is equivalent to the Lax–Wendroff scheme.

The truncation error for the grid function w has the form

$$\begin{aligned} Lw &= \frac{w_k^{n+1} - w_k^n}{\Delta t} + 2a \frac{w_k^n - w_{k-1}^n}{h(1 + \alpha)} + \left(1 - a \frac{\Delta t}{h} \right) a \frac{w_{k+1}^n - 2w_k^n + w_{k-1}^n}{h(1 + \alpha)} \\ &= q_t(x_k, t^n) + \frac{\Delta t}{2} q_{tt}(x_k, t^n) + a q_x(x_k, t^n) + \frac{1}{4} h(\alpha - 1) a q_{xx}(x_k, t^n) \\ &\quad - \frac{1}{4} h(1 + \alpha) a q_{xx}(x_k, t^n) \\ &\quad + \left(1 - a \frac{\Delta t}{h} \right) a \frac{\frac{1}{4} h^2(1 + \alpha)^2 q_{xx}(x_k, t^n) - \frac{1}{4} h^2(\alpha^2 - 1) q_{xx}(x_k, t^n)}{h(1 + \alpha)} + \mathcal{O}(\Delta t^2, h^2). \end{aligned}$$

Here we use $h_{k+\frac{1}{2}} = h_{k-\frac{1}{2}} = \frac{1}{2}h(1 + \alpha)$ for the distance from the cell center of the small cell k to the cell centers of the neighboring cells. By using the relations $q_t(x_k, t^n) = -a q_x(x_k, t^n)$ and $q_{tt}(x_k, t^n) = a^2 q_{xx}(x_k, t^n)$ all lower order terms in the above equation cancel and we obtain $Lw = \mathcal{O}(\Delta t^2, h^2)$. This shows that $|w_k - Q_k| = \mathcal{O}(\Delta t^2, h^2)$. Since the grid function was chosen to satisfy $w = q + \mathcal{O}(h^2)$, we conclude that

$$|q_k - Q_k| = \mathcal{O}(\Delta t^2, h^2).$$

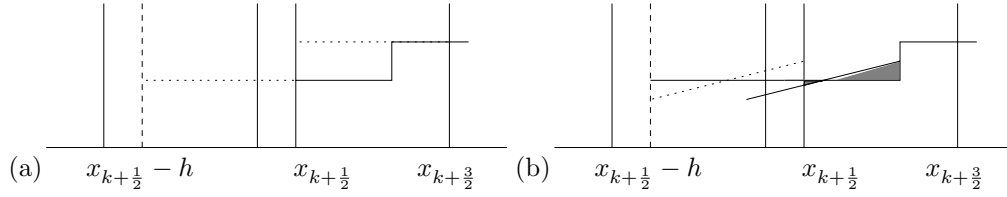


FIG. 2. h -box values at the interface $x_{k+\frac{1}{2}}$; dotted lines depict the initial values, solid lines the solution after one time step. (a) first order update by h -box method; (b) second order correction wave of $Q_{i+\frac{1}{2}}^L$.

Stability of this second order accurate scheme will be shown in the appendix.

Using the same grid function w , one can also show that $Lw = \mathcal{O}(\Delta t^2, h^2)$ in the neighboring grid cells $k - 1$ and $k + 1$. Therefore, the numerical solution converges with second order accuracy in the whole domain. \square

Figure 2 shows a schematic description of the first order update and the high-resolution correction for cell $k + 1$. The dotted lines depict the initial values, i.e., $Q_{k+\frac{1}{2}}^L$ and $Q_{k+\frac{1}{2}}^R = Q_{k+1}$. In a first step the piecewise constant values are propagated over a distance $a\Delta t$, as shown in Figure 2(a). In order to increase the accuracy, the piecewise constant initial values are replaced by piecewise linear functions. In Figure 2(b), we show the piecewise linear reconstructed function $Q_{k+1}^L(x, t^n)$ that has the slope $\sigma = (Q_{k+\frac{1}{2}}^R - Q_{k+\frac{1}{2}}^L)/h$. Since we already calculated the first order update, the second order correction terms, calculated by propagating piecewise linear initial values $Q_{k+\frac{1}{2}}^L(x, t^n)$ instead of the piecewise constant value $Q_{k+\frac{1}{2}}^L$, take only the shaded region shown in Figure 2(b) into account. Compare with LeVeque [17], where such second order correction terms were described for the approximation of the advection equation on a uniform grid.

3.3. Limiters for the h -box method. In order to have control over unphysical oscillations near discontinuities some kind of limiters must be used in the second order correction terms (2.4). In the wave propagation algorithm this is done by using *wave limiters* that modify the magnitude of the waves \mathcal{W}^p ($p = 1, \dots, M_w$) in the fluxes that model the second order correction terms. A limited p -wave $\mathcal{W}_{i+\frac{1}{2}}^p$ is obtained by comparison of this wave with the neighboring p -waves $\mathcal{W}_{i-\frac{1}{2}}^p$ or $\mathcal{W}_{i+\frac{3}{2}}^p$, depending on the direction of flow; see LeVeque [18] or [19] for details.

In our high-resolution h -box method we can use the same limiting process in order to obtain limited versions of the waves that were calculated from h -box values. These limited waves can then be used in the second order correction fluxes (3.8). In order to obtain the limiter for waves at a small cell interface, we compare those waves with waves arising from Riemann problems at a distance h away from the cell interface. This can be done by constructing two additional h -boxes at the small cell interface. The waves resulting from the solution of Riemann problems defined by these new h -box values to the left- and right-hand side of a small cell interface can then be used in order to estimate the wave limiter for the waves at the small cell interface. This requires the solution of two additional Riemann problems for each small cell interface; see Figure 3. We used such a limiting process in order to approximate a shock wave solution on an irregular grid shown in section 5.

In addition to the wave limiting process we also include a limiter into the approximation of the h -box values. Note that the h -box values (3.3) can also be obtained by

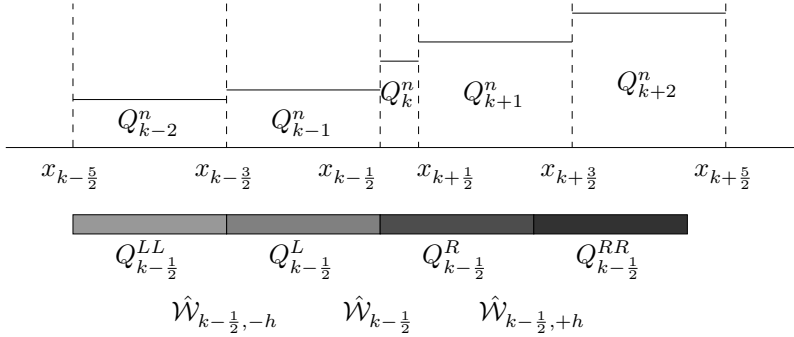


FIG. 3. Schematic description of h -box values assigned to the left small cell interface. Two additional h -box values are needed to estimate the wave limiter for the second order correction terms.

reconstructing a piecewise linear function $\bar{Q}(x)$ from the cell averages Q_i for all i and calculating the average value of this piecewise linear function over the same boxes of length h , as indicated in Figure 1. If the reconstructed function has the form

$$(3.9) \quad \bar{Q}_{k-1}(x) = Q_{k-1} + \frac{Q_k - Q_{k-1}}{\frac{1}{2}h(1 + \alpha)}(x - x_{k-1}) \quad \text{for } x \in [x_{k-3/2}, x_{k-1/2}),$$

$$(3.10) \quad \bar{Q}_{k+1}(x) = Q_{k+1} + \frac{Q_{k+1} - Q_k}{\frac{1}{2}h(1 + \alpha)}(x - x_{k+1}) \quad \text{for } x \in [x_{k+1/2}, x_{k+3/2}),$$

then averaging over boxes of length h leads to h -box values that have the form (3.3). The slopes of the piecewise linear initial values are

$$\sigma_{k-1} = \frac{Q_k - Q_{k-1}}{h(1 + \alpha)/2} \quad \text{and} \quad \sigma_{k+1} = \frac{Q_{k+1} - Q_k}{h(1 + \alpha)/2}.$$

Near discontinuities such piecewise linear values may not represent a good approximation of the solution. We can use standard *slope limiters* in order to obtain better approximations there. We can, for instance, use a slope limiter proposed by van Leer [29]. Here the slopes are replaced by limited versions that have the form $\hat{\sigma}_i = \sigma_i \phi_i$ for $i \in \{k - 1, k + 1\}$. For our application the limiter has the form

$$\phi_i(\theta_i) = \min \left(1, \frac{|\theta_i| + \theta_i}{1 + |\theta_i|} \right)$$

with

$$\theta_{k-1} = \frac{Q_{k-1} - Q_{k-2}}{Q_k - Q_{k-1}} \quad \text{and} \quad \theta_{k+1} = \frac{Q_{k+2} - Q_{k+1}}{Q_{k+1} - Q_k}.$$

It may be replaced by other limiter functions. Note that we do not want to use a steeper slope than σ_{k-1} (respectively, σ_{k+1}) for the construction of h -box values, because only those values lead to a second order approximation in smooth regions. However, near discontinuities we want to limit these slopes. The resulting limited h -box values can be calculated using the formulas

$$Q_{k+1/2}^L = \alpha Q_k + (1 - \alpha) \left(Q_{k-1} + \frac{\alpha}{1 + \alpha} (Q_k - Q_{k-1}) \phi_{k-1} \right),$$

$$Q_{k-1/2}^R = \alpha Q_k + (1 - \alpha) \left(Q_{k+1} + \frac{\alpha}{1 + \alpha} (Q_k - Q_{k+1}) \phi_{k+1} \right).$$

4. On the stability of the h -box method. The h -box method retains stability by constructing a finite volume scheme for which the flux difference is of the order of the size of the grid cell. For a small grid cell this requires $F_{k+\frac{1}{2}} - F_{k-\frac{1}{2}} = \mathcal{O}(\alpha h)$. In this case the term αh arising in the denominator of the finite volume scheme should not cause a stability problem. In regions where the solution of the conservation law is smooth, the h -box values are constructed to satisfy an analogous property, namely $Q_{k+\frac{1}{2}}^{L,R} - Q_{k-\frac{1}{2}}^{L,R} = \mathcal{O}(\alpha h)$. Since in our applications the flux function is a Lipschitz continuous function of Q^L and Q^R , the flux difference has the required cancellation property; see [5].

For the advection equation Stern [28] proved that the first order accurate h -box methods are TVD. Here we will briefly outline this proof which follows the general concept described above. The first order h -box method can (for $a > 0$) be rewritten in the form

$$\begin{aligned} Q_i^{n+1} &= Q_i^n - \frac{a\Delta t}{\alpha_i h} (Q_{i+\frac{1}{2}}^L - Q_{i-\frac{1}{2}}^L) \\ &= Q_i^n - \frac{a\Delta t}{\alpha_i h} \left(\alpha_i Q_i^n - \underbrace{\alpha_i \frac{1}{\alpha_i h} \int_{x_{i-\frac{1}{2}}-h}^{x_{i-\frac{1}{2}}-h+\alpha_i h} \bar{Q}_{i-1}^n(x) dx}_{\bar{Q}_i^n} \right). \end{aligned}$$

Here we assume that each grid cell has the size $h_i = \alpha_i h$, with $0 < \alpha_i \leq 1$. $\bar{Q}_{i-1}^n(x)$ is the piecewise linear reconstructed function (3.9). The stability result also holds on an irregular grid with more than one small cell. See also section 5 for a slightly different generalization of the piecewise linear function that has to be used in the construction of h -box values for a completely irregular grid.

Using this notation we now consider the difference $|Q_{i+1}^{n+1} - Q_i^{n+1}|$ and sum over all grid cells. This sum can be estimated as

$$\begin{aligned} TV(Q^{n+1}) &= \sum_i |Q_{i+1}^{n+1} - Q_i^{n+1}| \\ &\leq \left(1 - \frac{a\Delta t}{h}\right) \sum_i |Q_{i+1}^n - Q_i^n| + \frac{a\Delta t}{h} \sum_i |\bar{Q}_{i+1}^n - \bar{Q}_i^n|. \end{aligned}$$

We obtain the TVD property $TV(Q^{n+1}) \leq TV(Q^n)$ for time steps $CFL_h \leq 1$ if

$$(4.1) \quad \sum_i |\bar{Q}_{i+1}^n - \bar{Q}_i^n| \leq TV(Q^n).$$

For the h -box method (3.2) using h -box values that were calculated by averaging over piecewise constant values, (4.1) is always satisfied, since $\bar{Q}_i^n = Q_i^n$. For the more accurate first order h -box method (3.4), the TVD property can be shown if a TVD slope limiter is used in the construction of the h -box values, as discussed in section 3.3.

Note that for the approximation of the advection equation, the first order h -box method based on h -box values (3.1), i.e., defined by averaging over piecewise constant values of the conserved quantities, is also monotone. This property does not carry over to the first order h -box method with h -box values calculated by the interpolation formula (3.3). Note also that none of these two first order accurate h -box methods applied to Burgers's equation leads to a monotone method.

In the appendix we show stability for the second order accurate h -box method applied to the advection equation. This proof is based on the stability theory of Gustafsson, Kreiss, and Sundström [11].

5. Irregular grid calculation. In order to demonstrate the robustness of the high-resolution h -box method we now apply the scheme to a completely arbitrary grid; see Figure 4. By again assigning values to boxes of length h , we obtain a scheme that remains stable for time steps appropriate for a uniform grid with grid cells of length h . In this more general situation more than two grid cells may be overlapped by an h -box. We assume that grid cells have the length $h_i = \alpha_i h$, with $\alpha_i \leq 1$ for all indices i . We will show that a generalization of the h -box method based on averaging over piecewise linear values of the conserved quantities gives accurate results also in this more difficult situation. We will need to use piecewise linear reconstructed values

$$(5.1) \quad \bar{Q}_i(x) = Q_i + \frac{Q_{i+1} - Q_i}{h(\alpha_i + \alpha_{i+1})/2}(x - x_i) \quad \text{for } x \in [x_{i-\frac{1}{2}}, x_{i+\frac{1}{2}}), \quad i \in \{m, l\},$$

$$(5.2) \quad \bar{Q}_j(x) = Q_j + \frac{Q_j - Q_{j-1}}{h(\alpha_j + \alpha_{j-1})/2}(x - x_j) \quad \text{for } x \in [x_{j-\frac{1}{2}}, x_{j+\frac{1}{2}}), \quad j \in \{s, t\}.$$

The indices m, l and s, t indicate the grid cells that are only partly covered by the left- (respectively, right-) going h -boxes that are constructed at the cell interfaces of grid cell k . Slopes are needed only in these four cells because averaging over an entire cell gives a value that is independent of the slope. Averaging over these piecewise linear functions leads to the h -box values

$$(5.3) \quad \begin{aligned} Q_{k-\frac{1}{2}}^L &= \sum_{i=m+1}^{k-1} \alpha_i Q_i + \left(1 - \sum_{i=m+1}^{k-1} \alpha_i\right) \cdot \left[Q_m + \frac{Q_{m+1} - Q_m}{\alpha_m + \alpha_{m+1}} \left(\sum_{i=m}^{k-1} \alpha_i - 1\right)\right], \\ Q_{k-\frac{1}{2}}^R &= \sum_{i=k}^{s-1} \alpha_i Q_i + \left(1 - \sum_{i=k}^{s-1} \alpha_i\right) \cdot \left[Q_s + \frac{Q_s - Q_{s-1}}{\alpha_s + \alpha_{s-1}} \left(1 - \sum_{i=k}^s \alpha_i\right)\right], \\ Q_{k+\frac{1}{2}}^L &= \sum_{i=l+1}^k \alpha_i Q_i + \left(1 - \sum_{i=l+1}^k \alpha_i\right) \cdot \left[Q_l + \frac{Q_{l+1} - Q_l}{\alpha_l + \alpha_{l+1}} \left(\sum_{i=l}^k \alpha_i - 1\right)\right], \\ Q_{k+\frac{1}{2}}^R &= \sum_{i=k+1}^{t-1} \alpha_i Q_i + \left(1 - \sum_{i=k+1}^{t-1} \alpha_i\right) \cdot \left[Q_t + \frac{Q_t - Q_{t-1}}{\alpha_t + \alpha_{t-1}} \left(1 - \sum_{i=k+1}^t \alpha_i\right)\right]. \end{aligned}$$

5.1. Approximation of the advection equation on irregular grids. We can show that these h -box values used in an upwind scheme (which is equivalent to the first order wave propagation algorithm) lead to a consistent approximation of the advection equation.

PROPOSITION 3. *The h -box method $Q_i^{n+1} = Q_i^n - a \frac{\Delta t}{\alpha_i h} (Q_{i+\frac{1}{2}}^L - Q_{i-\frac{1}{2}}^L)$ with h -box values defined by (5.3) leads to a first order accurate approximation of the advection equation (with advection speed $a > 0$) on an irregular grid.*

The proof is based on Taylor series expansion and may be found in the preprint version of this paper [2]. Together with the stability result mentioned in section 4, we obtain first order convergence of this h -box method on irregular grids using time steps that satisfy $CFL_h \leq 1$.

Once the h -box values are defined we can apply the same second order correction terms (3.8) at the cell interfaces of a completely irregular grid. With such an approach

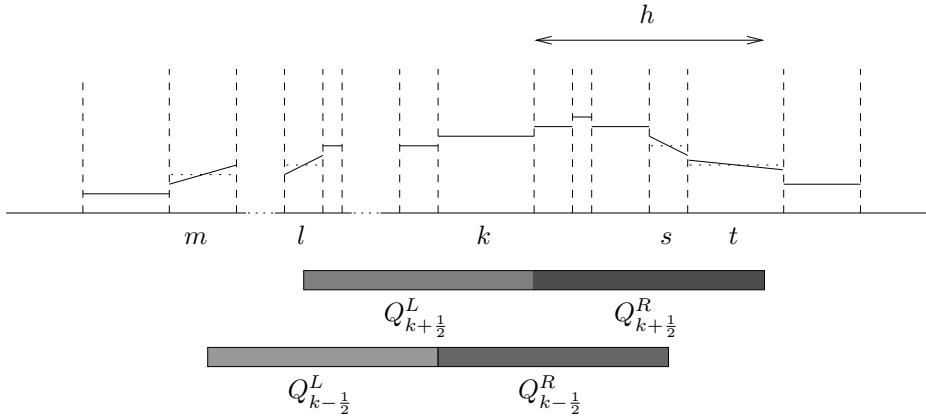


FIG. 4. Schematic description of the h -box method on a completely irregular grid.

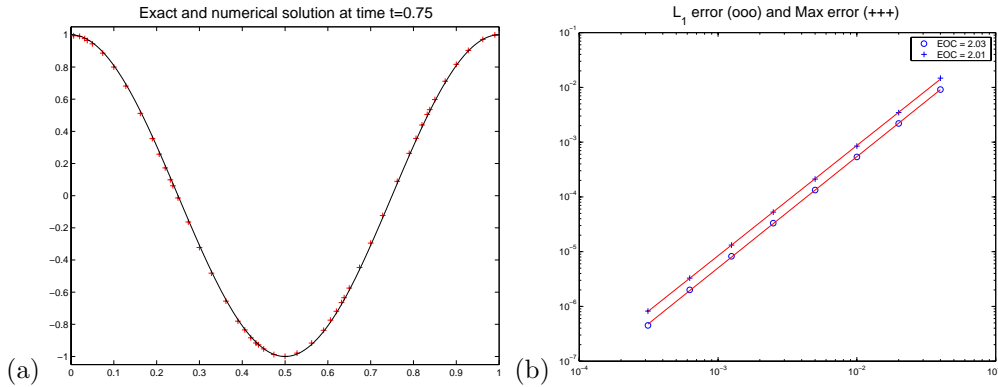


FIG. 5. Approximation of the advection equation on an irregular grid using the high-resolution h -box method with h -box values calculated by linear interpolation. (a) numerical results on an irregular grid with $h = 0.04$; (b) log-log-plot of h versus L_1 -norm error as well as maximum-norm error shows second order convergence.

we can expect second order convergence. Figure 5 shows numerical results for the approximation of the advection equation on a sequence of irregular grids. The initial values are set to $q(x, 0) = \sin(2\pi x)$ on the interval $[0, 1]$. Periodic boundary conditions are imposed. A convergence study shows that our new high-resolution h -box method converges with second order accuracy both in the L_1 -norm as well as the maximum norm. The accuracy of this calculation compares well with the accuracy of the standard wave propagation algorithm that was briefly described in section 2. However, here we could use much larger time steps. In Figure 6, we show results for the same test case, but here the h -box values were constructed by averaging over piecewise constant values of the conserved quantity, i.e., the formally inconsistent method described in section 3.1. Although we add second order correction terms (which increases the accuracy) the resulting method is only first order accurate. This is analogous to our analytical results for the simpler situation with only one small cell.

5.2. Approximation of the Euler equations on irregular grids. In this section we study the performance of the high-resolution h -box method for one-dimensional

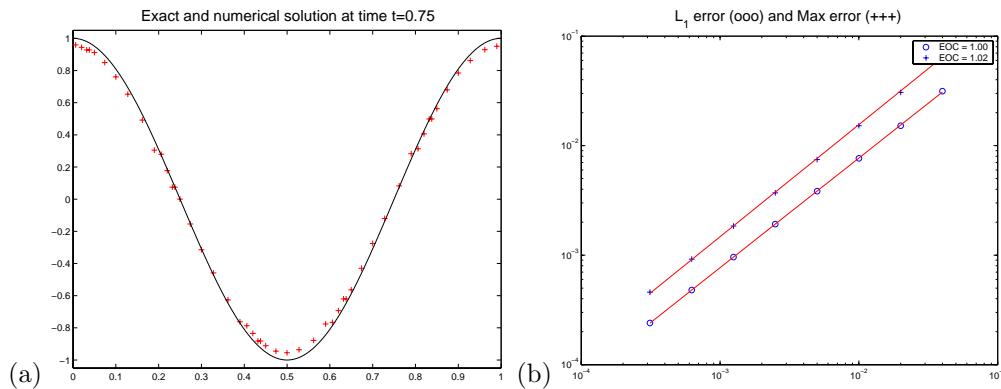


FIG. 6. Approximation of the advection equation on an irregular grid using an h -box method with second order correction terms, where h -box values are calculated by averaging over piecewise constant values of the conserved quantity. (a) numerical results on an irregular grid with $h = 0.04$; (b) log-log-plot of h versus L_1 -norm error as well as maximum-norm error shows first order convergence.

Euler equations. The equations can be written in the form (1.1) with

$$q = (\rho, \rho u, E), \quad f(q) = (\rho u, \rho u^2 + p, u(E + p)),$$

where ρ, p, E , and u describe the density, pressure, total energy, and the velocity, respectively. The equation of state has the form

$$E = \frac{p}{\gamma - 1} + \frac{1}{2}\rho u^2.$$

First we consider the approximation of a test problem defined in Example 5.1 on an irregular grid.

Example 5.1. We consider the numerical approximation of the one-dimensional Euler equations on an irregular grid. The grid cells vary in size between $h/10$ and h . The initial values are sufficiently smooth so that the solution does not develop shocks over the time interval considered. Reflecting boundary conditions are imposed on the left and right boundary. The computational domain is the interval $[0, 1]$. Our initial values are

$$\rho(x, 0) = 1 + 0.4 \sin\left(\frac{\pi}{2} + x\pi\right), \quad u(x, 0) = 0.25 - (x - 0.5)^2, \quad p(x, 0) = 1.$$

The ratio of specific heats is set to $\gamma = 1.4$.

In Figure 7 we show numerical results for the approximation of Example 5.1 using our new high-resolution h -box method. A convergence study for density at different time steps is shown in Table 5.1. Here we compare the numerical solution for density on a sequence of irregular grids to a highly resolved reference solution that was calculated on a regular spaced grid. We show results for both the unlimited second order h -box method and a version using the minmod limiter. Next we consider the approximation of a shock wave with the Euler equations.

Example 5.2. We consider the one-dimensional Euler equations with initial values on the interval $[0, 1]$ that have constant density $\rho = 1$ and constant pressure $p = 1$. The velocity is set to $u = 1$ for $x < 0.5$ and $u = -1$ for $x > 0.5$. The ratio of specific heats is $\gamma = 1.05$. The exact solution of this problem consists of two symmetric

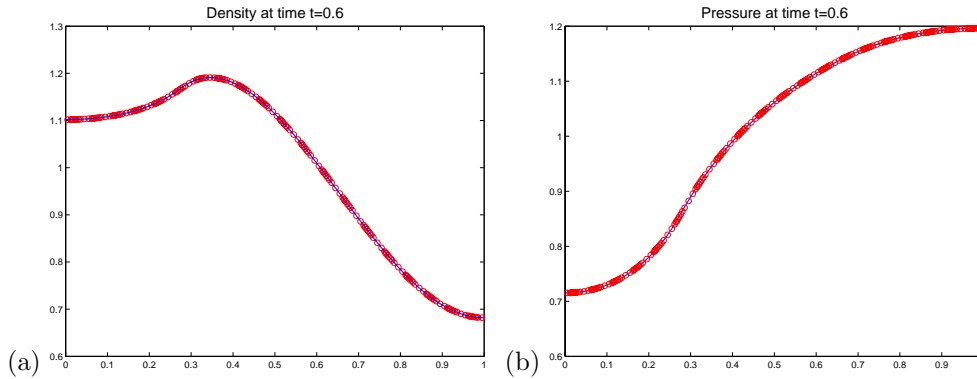


FIG. 7. Numerical results of density and pressure for Example 5.1 on an irregular grid ($h = 0.02$). The solid line shows a highly resolved reference solution calculated on a regular grid.

TABLE 5.1

Convergence study for Example 5.1. L_1 error of density at different times as well as the experimental order of convergence (EOC) are shown. For this smooth test problem, we show results for the unlimited second order h -box method as well as the limited h -box method using a minmod limiter.

	t=0.2	t = 0.4	t = 0.6	t = 0.8	t = 1
h /EOC	L_1 error of density (unlimited method)				
0.02	1.1229d-4	1.544d-4	3.4573d-4	5.9017d-4	0.0014
0.01	2.9567d-5	4.2550d-5	9.4628d-5	1.7825d-4	4.2628d-4
EOC	1.92	1.86	1.87	1.73	1.72
0.005	7.7282d-6	1.1786d-5	2.5092d-5	5.1242d-5	1.3381d-4
EOC	1.94	1.89	1.91	1.80	1.67
h /EOC	L_1 error of density (using minmod limiter)				
0.02	1.6893d-4	2.0212d-4	3.1620d-4	5.2083d-4	0.0012
0.01	5.6937d-5	6.5761d-5	1.1105d-4	1.9282d-4	3.6960d-4
EOC	1.57	1.62	1.51	1.46	1.70
0.005	1.6357d-5	2.1260d-5	4.5036d-5	7.6802d-5	1.2018d-4
EOC	1.80	1.63	1.30	1.33	1.62

shock waves that are propagating outwards. We use an irregular grid with grid cells that may be smaller than $h = 0.01$ on the left half of the interval. For $x > 0.5$ the grid is regular with mesh length $\Delta x = 0.01$. We use time steps that correspond to $CFL_h \approx 0.9$.

Figure 8 shows numerical results of Example 5.2 for the high-resolution h -box method based on the linear interpolation formula. Our numerical results in Figure 8(a) show that the limiters described in section 3.3 can suppress spurious oscillations near the discontinuity. The approximation of the shock wave that is moving into the region of the irregular grid is in good agreement with the symmetric shock wave that is moving into the regular part of the grid. On the irregular grid the shock is smeared out over more grid cells than on the regular grid. The reason for this more smeared out shock profile is that a jump in the conserved quantities can influence several h -box values. In Figure 8(b) we show the results obtained by the second order method without limiters.

6. Approximation of transonic rarefaction waves. In this section we point out that h -box methods can cause numerical difficulties in the approximation of tran-

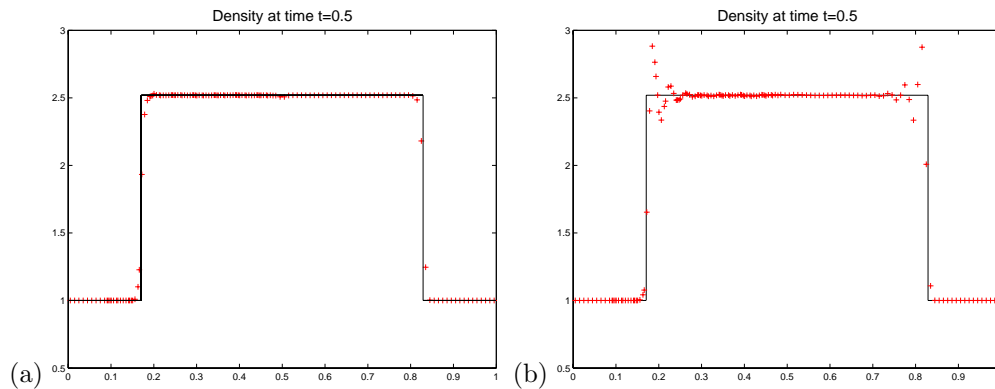


FIG. 8. Approximation of Example 5.2 on a grid that is irregular for $x < 0.5$ and regular for $x > 0.5$. (a) plot of density with limiters; (b) plot of density without limiters. The solid line indicates the exact solution.

sonic rarefaction waves that do not appear for standard Godunov-type methods on regular or irregular spaced grids. To see this we first consider the approximation of Burgers's equation $q_t + (q^2/2)_x = 0$ with initial values $q(x, 0) = -0.5$ for $x \leq 0.5$ and $q(x, 0) = 0.5$ for $x > 0.5$ on an irregular grid. The first order accurate fluxes at the cell interface $x_{i-\frac{1}{2}}$ can be calculated by using the exact formula, i.e.,

$$F_{i-\frac{1}{2}} = \begin{cases} \min_{Q_{i-\frac{1}{2}}^L \leq q \leq Q_{i-\frac{1}{2}}^R} f(q) & : Q_{i-\frac{1}{2}}^L \leq Q_{i-\frac{1}{2}}^R, \\ \max_{Q_{i-\frac{1}{2}}^R \leq q \leq Q_{i-\frac{1}{2}}^L} f(q) & : Q_{i-\frac{1}{2}}^R \leq Q_{i-\frac{1}{2}}^L, \end{cases}$$

with the flux $f(q) = \frac{1}{2}q^2$. Figure 9(a) demonstrates that this method produces unphysical oscillations around the sonic point. Note that in this section we use only first order accurate methods to isolate this phenomenon from the flux limiting procedure. The numerical problem can be avoided by using the Lax–Friedrichs flux, which has at the interface $x_{i-\frac{1}{2}}$ the form

$$F_{i-\frac{1}{2}} = \frac{1}{2}(f(Q_{i-\frac{1}{2}}^L) + f(Q_{i-\frac{1}{2}}^R)) + \frac{h}{2\Delta t}(Q_{i-\frac{1}{2}}^L - Q_{i-\frac{1}{2}}^R).$$

See Figure 9(b) for numerical results.

The same effect can also be observed in the approximation of a transonic rarefaction wave for the Euler equations. To see this we consider a shock tube problem for which the solution consists of a right-moving shock wave, a contact discontinuity, and a left-moving transonic rarefaction wave. The initial values are $\rho = 1$, $u = 0.75$, $p = 1$ for $x \leq 0.3$ and $\rho = 0.125$, $u = 0$, $p = 0.1$ for $x > 0.3$. The ratio of specific heats is $\gamma = 1.4$. For the numerical approximation we used a Roe–Riemann solver with standard entropy fix for transonic rarefaction waves. The results of this calculation are shown in Figure 10. The numerical solution shows some oscillations around the sonic point; see Figure 10(b) for a closer view of the region around the sonic point. If the fluxes at the cell interfaces are again calculated by the Lax–Friedrichs method this numerical problem does not arise; see Figure 11.

In the preprint [2] of this paper, we studied the entropy consistency of the h -box method for the approximation of Burgers's equation. For the h -box method with Godunov flux, we showed that a discrete entropy inequality is satisfied away from sonic

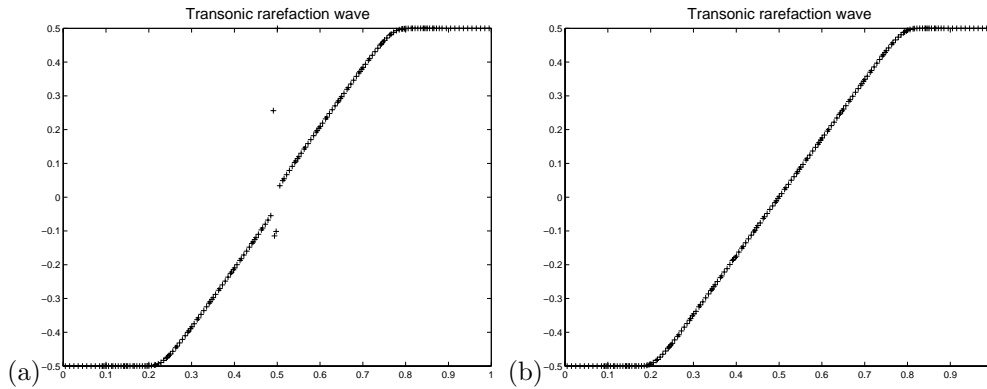


FIG. 9. Approximation of a transonic rarefaction wave solution for Burgers's equation on an irregular grid. (a) *h*-box method based on Godunov flux; (b) *h*-box method based on Lax-Friedrichs flux.

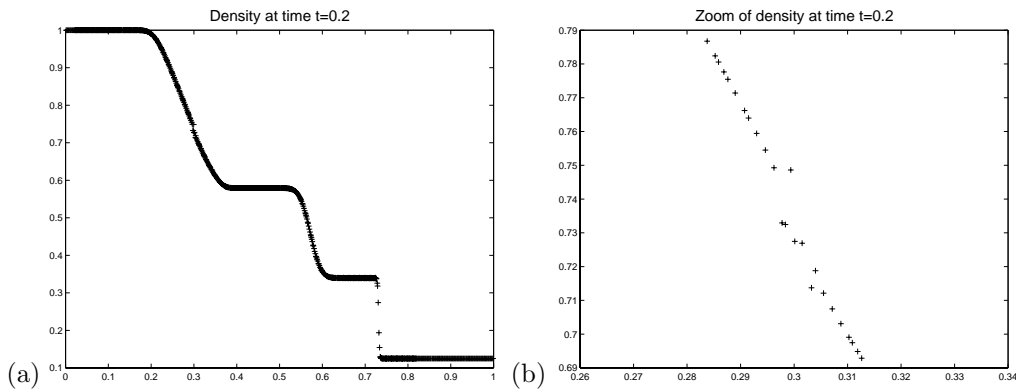


FIG. 10. Approximation of a shock tube problem for the Euler equations. (a) plot of density obtained by first order Roe solver with entropy fix; (b) zoom of density around sonic point.

points. This implies that the numerical solution converges to the entropy consistent weak solution of the conservation law. We showed that this discrete entropy inequality can be violated at a sonic point. While this does not give us any prediction whether or not the method is entropy consistent at the sonic point, it is interesting to note that this is exactly the case where the *h*-box method leads to numerical difficulties. We plan to further investigate the entropy consistency of *h*-box methods in order to develop an entropy fix that is less dissipative than the Lax-Friedrichs method and that can be extended to a high-resolution method.

7. Higher-dimensional irregular grid calculations. Now we will consider two-dimensional systems of conservation laws in the form

$$(7.1) \quad \frac{\partial}{\partial t} q(x, y, t) + \frac{\partial}{\partial x} f(q(x, y, t)) + \frac{\partial}{\partial y} g(q(x, y, t)) = 0.$$

The simplest way to extend a one-dimensional method for conservation laws to multidimensional problems is to use dimension splitting. Equation (7.1) would be approximated by solving one-dimensional subproblems in an alternating way. The high-resolution one-dimensional *h*-box method could be used in each substep.

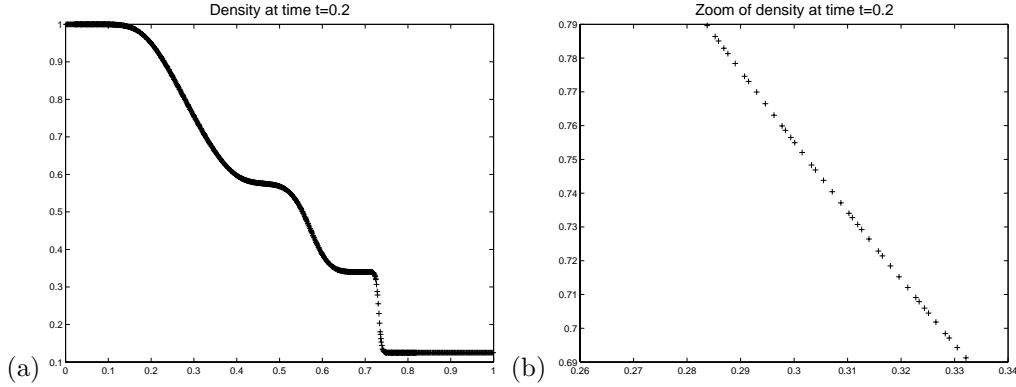


FIG. 11. Approximation of a shock tube problem for the Euler equations. (a) plot of density obtained by Lax-Friedrichs method; (b) zoom of density around sonic point.

Instead of using a dimensional splitting approach, we will here develop a two-dimensional h -box method that is based on the multidimensional wave propagation algorithm [17], [18]. We assume that the reader is familiar with the two-dimensional wave propagation algorithm and with the notation used below. As a first step in this approach we solve one-dimensional Riemann problems normal to each cell interface. Based on formula (3.6), which describes the one-dimensional h -box method, we obtain

$$\begin{aligned}
 Q_{ij}^{n+1} &= Q_{ij}^n + \Delta_{ij}^{up} \\
 (7.2) \quad &= Q_{ij}^n - \frac{\Delta t}{\Delta x_i} \left(\mathcal{A}^+ \Delta \hat{Q}_{i-\frac{1}{2},j} + \mathcal{A}^- \Delta \hat{Q}_{i+\frac{1}{2},j} + f(Q_{i+\frac{1}{2},j}^L) - f(Q_{i-\frac{1}{2},j}^R) \right) \\
 &\quad - \frac{\Delta t}{\Delta y_j} \left(\mathcal{B}^+ \Delta \hat{Q}_{i,j-\frac{1}{2}} + \mathcal{B}^- \Delta \hat{Q}_{i,j+\frac{1}{2}} + g(Q_{i,j+\frac{1}{2}}^L) - g(Q_{i,j-\frac{1}{2}}^R) \right).
 \end{aligned}$$

The method (7.2) is stable for time steps that satisfy $CFL_h \leq \frac{1}{2}$. Second order correction terms of the form (3.8) can be included in x as well as in y direction, which leads to a method of the form

$$(7.3) \quad Q_{ij}^{n+1} = Q_{ij}^n + \Delta_{ij}^{up} - \frac{\Delta t}{\Delta x_i} \left(\hat{F}_{i+\frac{1}{2},j}^2 - \hat{F}_{i-\frac{1}{2},j}^2 \right) + \frac{\Delta t}{\Delta y_j} \left(\hat{G}_{i,j+\frac{1}{2}}^2 - \hat{G}_{i,j-\frac{1}{2}}^2 \right).$$

The second order correction terms are again obtained by using the waves and speeds calculated from solving Riemann problems defined by h -box values. Limiters are used in exactly the same form as described earlier for the one-dimensional case.

In addition to fluxes in the normal direction, the multidimensional wave propagation algorithm also calculates waves that are moving in a transverse direction. For the usual wave propagation scheme one has $Q_{i+\frac{1}{2},j}^L = Q_{i-\frac{1}{2},j}^R$ and $Q_{i,j+\frac{1}{2}}^L = Q_{i,j-\frac{1}{2}}^R$. In this case the transverse propagation of waves can be obtained by a decomposition of the flux differences $\mathcal{A}^\pm \Delta Q$, $\mathcal{B}^\pm \Delta Q$ into transverse fluctuations. For the h -box method this transverse propagation has to be modified. In order to explain the transverse propagation we consider the two-dimensional advection equation

$$\frac{\partial}{\partial t} q(x, y, t) + a \frac{\partial}{\partial x} q(x, y, t) + b \frac{\partial}{\partial y} q(x, y, t) = 0, \quad a, b > 0.$$

Assuming first that $\Delta x_i = h$ and $\Delta y_j \leq h$, the change of the cell average of the conserved quantity q in grid cell (i, j) due to the first order update in the x -direction

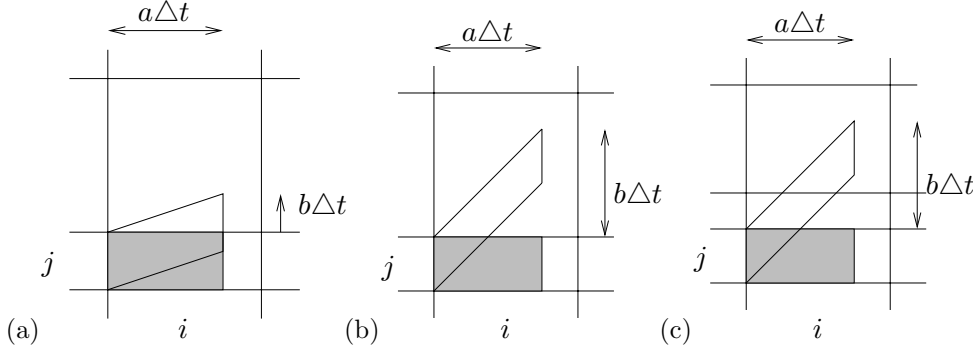


FIG. 12. Different possibilities for transverse propagation of a right-moving wave for the advection equation on a nonuniform Cartesian grid.

has the form

$$(7.4) \quad -\frac{\Delta t}{\Delta x_i} \mathcal{A}^+ \Delta Q_{i-\frac{1}{2},j} = -\frac{\Delta t}{h} a(Q_{i,j}^n - Q_{i-1,j}^n).$$

Since we assume that the advection speed a in the x -direction is positive, there is no wave that moves into this cell from the right cell interface. Furthermore, the difference $f(Q_{i+\frac{1}{2},j}^L) - f(Q_{i-\frac{1}{2},j}^R)$ vanishes in the case $\Delta x_i = h$. In the two-dimensional case a part of the right-moving flux difference $\mathcal{A}^+ \Delta Q$ should affect other grid cells. This is indicated in Figure 12. The shaded regions indicate the influence of the jump $Q_{ij} - Q_{i-1,j}$ (initially located at the left cell interface) due to the solution of the Riemann problem in the normal direction. In a multidimensional method the solution of the Riemann problem at the interface $x_{i-\frac{1}{2}}$ should not affect only the cell average of the conserved quantities in the grid cell $(i-1, j)$ and (i, j) . It should also have an effect on grid cells in the tangential direction. In the situation shown in Figure 12(a), the triangular portion of the wave describes the fraction that should affect the grid cell $(i, j+1)$. The transverse propagation of the wave considered in Figure 12(a) should change the cell average of the conserved quantity in grid cell (i, j) by the amount

$$\frac{(\Delta t)^2}{\Delta x_i \Delta y_j} \frac{1}{2} b \mathcal{A}^+ \Delta Q_{i-\frac{1}{2},j} = \frac{(\Delta t)^2}{\Delta x_i \Delta y_j} \frac{1}{2} \mathcal{B}^+ \mathcal{A}^+ \Delta Q_{i-\frac{1}{2},j}.$$

The change of the cell average of the conserved quantity in cell $(i, j+1)$ due to the transverse propagation of this wave has the form

$$-\frac{(\Delta t)^2}{\Delta x_i \Delta y_{j+1}} \frac{1}{2} \mathcal{B}^+ \mathcal{A}^+ \Delta Q_{i-\frac{1}{2},j}.$$

The notation $\mathcal{B}^\pm \mathcal{A}^\pm \Delta Q$ was introduced in [18] to describe transverse propagations of left- and right-moving flux differences. For the wave propagation algorithm with time step restriction $\text{CFL} \leq 1$ the transverse propagation has always the triangular form depicted in Figure 12(a), even if the grid is irregular. Since the transverse propagation approximates terms that are needed in order to obtain second order accuracy, we include those terms into the second order correction terms used in (7.3). The up-going flux difference $\mathcal{B}^+ \mathcal{A}^+ \Delta Q_{i-\frac{1}{2}}$ contributes to the \hat{G} term in the form of an update

$$\hat{G}_{i,j+\frac{1}{2}}^2 := \hat{G}_{i,j+\frac{1}{2}}^2 - \frac{1}{2} \frac{\Delta t}{\Delta x_i} \mathcal{B}^+ \mathcal{A}^+ \Delta Q_{i-\frac{1}{2},j}.$$

For our h -box method we have to extend the transverse propagation to allow also wave propagation of other forms, for instance those shown in Figures 12(b) or (c). For the situation shown in Figure 12(b) the update of the flux \tilde{G} due to the transverse propagation has the form

$$\hat{G}_{i,j+\frac{1}{2}}^2 := \hat{G}_{i,j+\frac{1}{2}}^2 - \frac{\Delta t - \frac{1}{2}\Delta y_j/b}{b\Delta t\Delta x_i} \Delta y_j \mathcal{B}^+ \mathcal{A}^+ \Delta Q_{i-\frac{1}{2},j}.$$

In the situation shown in Figure 12(c), the transverse propagation of $\mathcal{A}^+ \Delta Q_{i-\frac{1}{2},j}$ leads to an update of $\hat{G}_{i,j+\frac{1}{2}}^2$ as well as $\hat{G}_{i,j+\frac{3}{2}}^2$, depending on the fraction of the wave considered. As demonstrated in these examples, simple geometric routines can be used to calculate the fraction of the waves that determine the change of the cell average of the conserved quantity due to the transverse propagation. Note that the wave speed in the normal direction (i.e., a in our example) is present in the fluctuations $\mathcal{A}^\pm \Delta Q$. In order to calculate the transverse propagations no other information from the structure of the Riemann problem in the normal direction is needed. Therefore, even for a system of conservation laws, we have only to decompose the left- and right-moving flux differences, instead of decomposing each wave resulting from the Riemann problem in the normal direction separately.

So far we have assumed that $\Delta x_i = h$. If $\Delta x_i < h$, we want to use the one-dimensional h -box method in order to calculate the fluxes in the normal direction. The transverse propagation will take a very similar form as discussed above. Now we could interpret the grid cells (i, j) , $(i, j + 1)$ shown in Figure 12 as h -boxes constructed at the interface $x_{i-\frac{1}{2}}$. The transverse propagation of waves should again depend on the fraction of the wave that moves through the h -box considered. This can be calculated in exactly the same way as described above for the case $\Delta x_i = h$. In order to obtain the correct cancellation property needed for a stable update, we have to include the terms $f(Q_{i+\frac{1}{2},j}^L)$ and $f(Q_{i-\frac{1}{2},j}^R)$ that arise in (7.2) into our transverse propagation. Motivated by (2.1), (2.2) we do this by applying an update of the form

$$\begin{aligned} \mathcal{A}^+ \Delta Q_{i-\frac{1}{2},j} &:= \mathcal{A}^+ \Delta Q_{i-\frac{1}{2},j} - f(Q_{i-\frac{1}{2}}^R), \\ \mathcal{A}^- \Delta Q_{i-\frac{1}{2},j} &:= \mathcal{A}^- \Delta Q_{i-\frac{1}{2},j} + f(Q_{i-\frac{1}{2}}^L) \end{aligned}$$

before we calculate the change of the fluxes \hat{G}^2 . For our example of the advection equation with positive advection speeds, this update of $\mathcal{A}^\pm \Delta Q$ has the effect that $\mathcal{A}^- \Delta Q$ is no longer equal to zero. Moreover, the fraction of the wave that is propagated in the transverse direction depends only on the size of the grid cells and the speed b . Therefore, our transverse propagation has the effect that a fraction of the update used in (7.3) is propagated in the transverse direction. The update, which describes the wave propagation in the x -direction was already constructed to be of the order $\mathcal{O}(\Delta x)$ with $\Delta x \leq h$. Our transverse propagation allows that at most a fraction of magnitude $\mathcal{O}(\Delta y)$ ($\Delta y \leq h$) is propagated in the transverse direction. (See, for instance, Figure 12(c).) Therefore, our transverse propagation satisfies the cancellation property. The transverse propagation of $\mathcal{B}^+ \Delta Q$ also has to be included in an analogous way. By including the transverse propagation into our two-dimensional h -box method, we obtain stability for time steps that satisfy the condition $\text{CFL}_h \leq 1$.

A transverse propagation of the second order correction (3.8) can be included into the transverse propagation in the same form as it was discussed for the wave propagation algorithm in [18]. This further increases the accuracy of the method. It was used in our test calculations below.

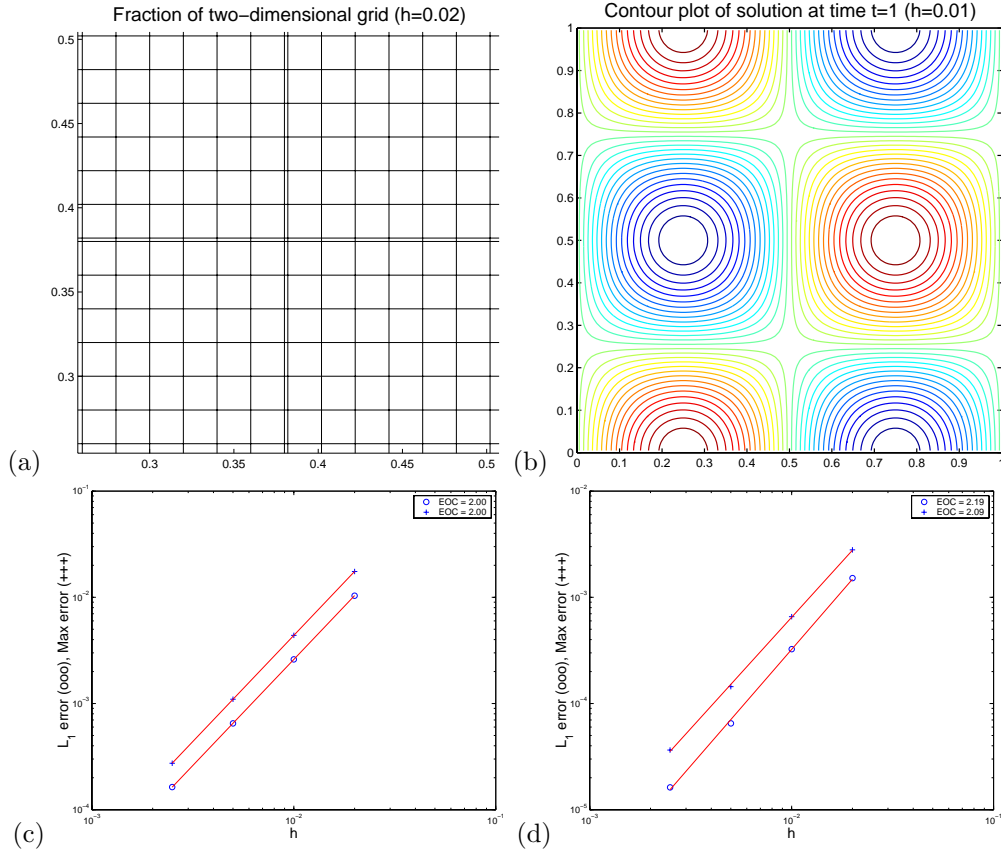


FIG. 13. Approximation of Example 7.1. (a) The grid for a discretization with $h = 0.02$; (b) contour plot of the solution using the two-dimensional h -box approach with $h = 0.01$ and $CFL_h \approx 0.9$; (c) convergence study for irregular grid CLAWPACK algorithm, $CFL \approx 0.9$; (d) convergence study for h -box method, $CFL_h \approx 0.9$ (o-symbol: error in L_1 -norm; +-symbol: error in maximum norm).

We now demonstrate the performance of our two-dimensional high-resolution h -box method for the approximation of the advection equation. We will compare the numerical results obtained for this h -box scheme with results obtained using the standard high-resolution CLAWPACK algorithm for irregular grid calculations. The latter method requires the time step restriction $CFL \leq 1$, while the h -box method is stable for time steps that satisfy $CFL_h \leq 1$. We first study the accuracy for the two-dimensional advection equation.

Example 7.1. We consider the approximation of the advection equation $q_t + q_x + q_y = 0$, with initial values $q(x, y, 0) = \sin(2\pi x) \cos(2\pi y)$ on the domain $[0, 1] \times [0, 1]$. We impose periodic boundary conditions. The grid contains two lines as well as two columns of grid cells with height (respectively, width) $0.1h$ and $0.9h$. All other grid cells have the size $h \times h$. See Figure 13(a) for a plot of a fraction of the grid.

Test calculations for Example 7.1 confirm that the h -box method leads to second order accurate approximations also in this multidimensional application. In Figure 13(d) we document the experimental order of convergence of the h -box method in both the L_1 -norm (depicted by o-symbols) as well as in the maximum norm (+-symbols). For this grid, inaccuracies near the small cells would be displayed in the

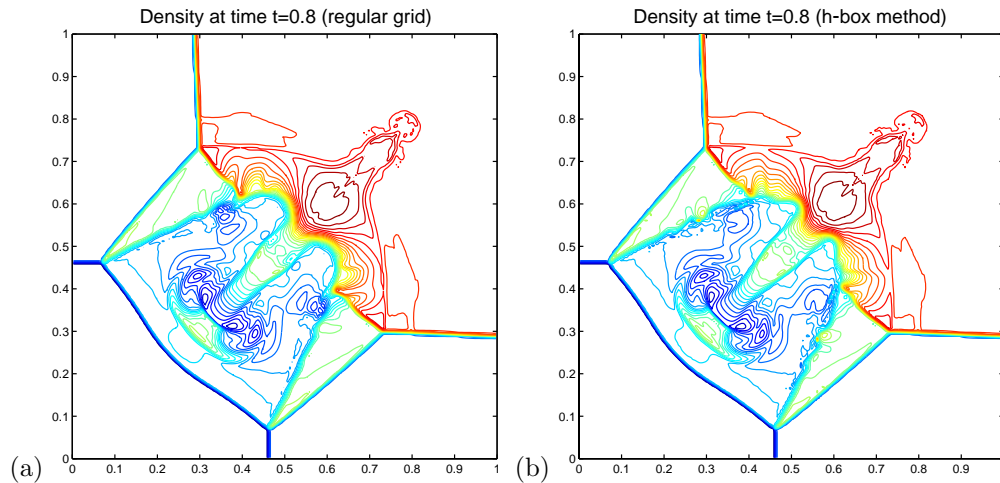


FIG. 14. (a) Contour plot of density obtained by the high-resolution wave propagation algorithm on a uniform grid with $h = 0.005$; (b) contour plot of density obtained with high-resolution h -box method, $h = 0.005$. We used the monotonized centered limiter.

maximum norm rather than in the L_1 -norm. However, in both norms the experimental order of convergence is about 2. The results for the h -box method compare well with numerical results obtained with the standard wave propagation algorithm with appropriate modifications that allow the approximation on a nonuniform grid. Both schemes converge with second order, but the error is slightly smaller if we use the h -box method. This is due to the numerical viscosity, since the time step restriction $\text{CFL} \approx 0.9$ for the wave propagation algorithm leads away from the small cell to time steps that correspond to $\text{CFL} \leq 0.1$.

Our two-dimensional h -box method can be extended to systems of conservation laws in the same way as the standard wave propagation algorithm. The modifications described above now have to be applied to each wave resulting from the decomposition of the left- (respectively, right-) going flux differences into up- and down-going waves. In our last example we consider the approximation of a two-dimensional Riemann problem for the Euler equations, as studied in [27]. This same example was considered in [18], where results of CLAWPACK calculations on a uniform grid are shown. The initial values are piecewise constant in four quadrants, and the solution of each single Riemann problem is a shock wave. Due to the interaction a complex solution structure is obtained. For this calculation we have, in addition to the regular grid cells of the size $h \times h$, 10 lines and 10 columns with height (respectively, width) varying between $0.1h$ and $0.9h$. Our solution on a nonuniform grid calculated by the high-resolution h -box method with $h = 0.005$ compares well with those obtained on a regular grid; see Figure 14. The shock waves are equally well approximated with both methods. Slight differences are visible only at the unstable contact lines, which are very sensitive to the numerical method; see also [18], where it was shown that different limiters have quite a large impact on the approximation.

8. Conclusions. We studied high-resolution h -box methods for the approximation of hyperbolic systems of conservation laws on irregular grids and showed that the definition of the h -box values is important in order to construct accurate schemes. In forthcoming work we will use this to construct a new two-dimensional high-resolution

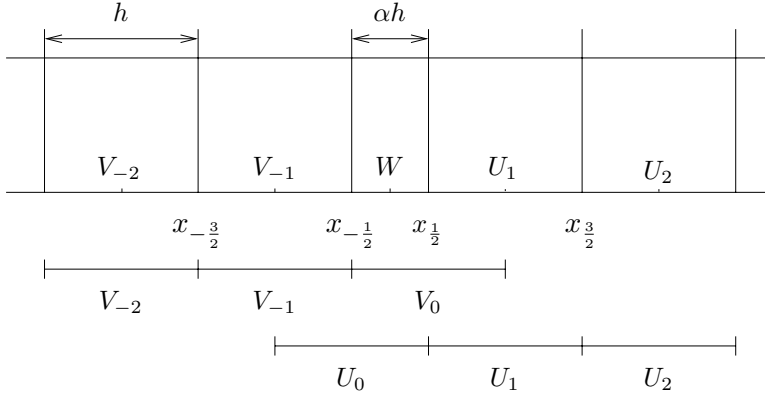


FIG. 15. Notation for GKS stability, with one small cell in the middle.

h -box scheme for the approximation of conservation laws with embedded irregular boundaries. So far there is no Cartesian grid embedded boundary method that leads to a second order accurate approximation at boundary cells. Further work will also concentrate on the entropy consistency of h -box methods and the approximation of transonic rarefaction waves.

Appendix A. Stability of the second order h -box method. In this appendix we prove the stability of the second order h -box scheme for $q_t = q_x$ using linear interpolation according to the theory of Gustafsson, Kreiss, and Sundström [11] (henceforth GKS). We treat the small cell with mesh width αh as a boundary condition for the Lax–Wendroff scheme applied on either side of the small cell, using the notation of Figure 15. Here the conserved quantity assigned to the right h -box at the interface $x_{-\frac{1}{2}}$ is denoted by V_0 . The left h -box value at the interface $x_{\frac{1}{2}}$ is U_0 . The derivation of the stability condition for the update of the small cell is similar to those used in Berger [1], where stability for schemes with local grid refinement was analyzed.

Both U and V are computed using the second order Lax–Wendroff scheme,

$$(A.1) \quad \begin{aligned} U_j^{n+1} &= U_j^n + \lambda/2(U_{j+1}^n - U_{j-1}^n) + \lambda^2/2(U_{j+1}^n - 2U_j^n + U_{j-1}^n), & j \geq 1, \\ V_j^{n+1} &= V_j^n + \lambda/2(V_{j+1}^n - V_{j-1}^n) + \lambda^2/2(V_{j+1}^n - 2V_j^n + V_{j-1}^n), & j \leq -1, \end{aligned}$$

with $\lambda = \frac{\Delta t}{h}$. Using the approach of [1], we look for solutions of the form

$$(A.2) \quad \begin{aligned} U_j^n &= \rho \kappa^j z^n, \quad |\kappa| \leq 1, & j = 1, 2, \dots, \\ V_j^n &= \sigma \tau^j z^n, \quad |\tau| \geq 1, & j = -1, -2, \dots \end{aligned}$$

With this numbering, for l_2 solutions the root κ of the characteristic equation for U on the right side has magnitude less than 1, and τ has magnitude greater than 1. Roughly speaking, the scheme is unstable if and only if there are l_2 solutions satisfying the interpolation conditions with growth in time $|z| > 1$.

The linear interpolation conditions (3.3) give us

$$(A.3) \quad U_0 = \frac{1-\alpha}{1+\alpha} V_{-1} + \frac{2\alpha}{1+\alpha} W, \quad V_0 = \frac{1-\alpha}{1+\alpha} U_1 + \frac{2\alpha}{1+\alpha} W,$$

where the small cell, labeled W above, satisfies the “small cell” version of Lax–Wendroff,

$$(A.4) \quad W^{n+1} = W^n + \frac{\Delta t}{\alpha h} \left[\frac{U_0 + U_1}{2} + \frac{\Delta t}{2h}(U_1 - U_0) - \frac{V_0 + V_{-1}}{2} - \frac{\Delta t}{2h}(V_0 - V_{-1}) \right].$$

The characteristic equation for W is $W^n = \hat{w}z^n$. We normalize the equations and take $\hat{w} = 1$. Substituting the characteristic roots for U, V into the interpolation conditions (A.3) gives

$$(A.5) \quad \rho = \frac{1 - \alpha}{1 + \alpha} \sigma \tau^{-1} + \frac{2\alpha}{1 + \alpha}, \quad \sigma = \frac{1 - \alpha}{1 + \alpha} \rho \kappa + \frac{2\alpha}{1 + \alpha}.$$

Equation (A.5) is easily solved for ρ and σ , giving

$$(A.6) \quad \rho = \frac{2\alpha(1 + \alpha + (1 - \alpha)\tau^{-1})}{(1 + \alpha)^2 - (1 - \alpha)^2 \kappa \tau^{-1}}, \quad \sigma = \frac{2\alpha(1 + \alpha + (1 - \alpha)\kappa)}{(1 + \alpha)^2 - (1 - \alpha)^2 \kappa \tau^{-1}}.$$

Substitution of the resolvent equations for U and V into (A.4) gives

$$(A.7) \quad z = 1 + \frac{\lambda}{2\alpha} [\rho(1 + \kappa) + \lambda\rho(\kappa - 1) - \sigma(1 + \tau^{-1}) - \lambda\sigma(1 - \tau^{-1})].$$

We use (A.5) to replace ρ and σ in terms of $\sigma\tau^{-1}$ and $\rho\kappa$. Also, for a given mesh width h on both the left and right, it is easily seen that the product of the roots κ and τ are $\kappa\tau = \frac{\lambda-1}{\lambda+1}$, so τ^{-1} can be replaced using κ . Thus, (A.7) simplifies to

$$(A.8) \quad z = 1 - \frac{2\lambda^2}{1 + \alpha} + \frac{\lambda(1 + \lambda)}{1 + \alpha} \kappa(\rho + \sigma).$$

We call this *root condition* for the stability of the small cell scheme with Lax–Wendroff. If there are roots z with $|z| > 1$ and κ, τ^{-1} with magnitude less than or equal to 1, satisfying (A.8), then by the GKS theory the scheme is unstable. Conversely, if there are no such roots, the scheme is stable. As in [1], we will use the maximum principle to reduce the range of values we need to check for stability.

To see that the maximum principle applies, we will show that the right-hand side of (A.8), call it $f(z)$, has no singularities for $|z| \geq 1$ and is bounded as $z \rightarrow \infty$. First note that $f(z) = (1 - \frac{2\lambda^2}{1+\alpha}) + \frac{\lambda(1+\lambda)}{1+\alpha} \kappa(\rho + \sigma)$ has no branch points for $|z| \geq 1$. This is because the roots κ, τ satisfy the Lax–Wendroff characteristic equation for (A.1),

$$(A.9) \quad z = 1 + \frac{\lambda}{2}(\eta - \eta^{-1}) + \frac{\lambda^2}{2}(\eta - 2 + \eta^{-1}),$$

which lead to a quadratic equation for η with roots

$$(A.10) \quad \eta_{1,2} = \frac{z - 1 + \lambda^2 \pm \sqrt{(z - 1)^2 + \lambda^2(2z - 1)}}{\lambda(\lambda + 1)}.$$

One of the roots is always inside the unit circle, and the other one is outside the unit circle; see [11, Lemma 6.1]. The root inside the unit circle is the root we call κ above, and τ is the root that is outside the unit circle.

The square root term of (A.10) is zero only for $z = 1 - \lambda$, which being inside the unit circle is outside the region of interest, so there are no branch points for $|z| > 1$.

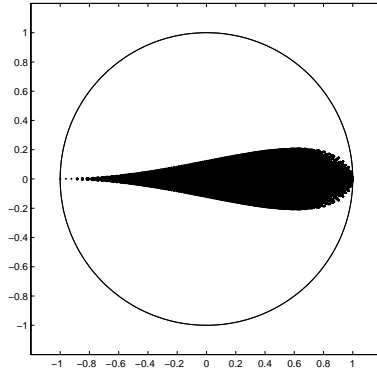


FIG. 16. Locus of values of $f(z)$ for $|z| = 1$; all values lie inside or on the unit circle.

Also, note from (A.10) that as $z \rightarrow \infty$, the root τ grows like $\frac{2z}{\lambda^2 + \lambda}$, so the root κ grows like $\frac{\lambda(\lambda-1)}{2z}$, which is clearly bounded for large z . So the maximum principle applies.

Thus $f(z)$ attains its maximum value on the circle $|z| = 1$. The next step then is to examine the magnitude of $f(z)$ for values of z on the unit circle. Since we can show only analytically that $f(z) \leq 1$ for $\lambda > 0.5$, we instead evaluate $f(z)$ numerically, for $0 \leq \alpha \leq 1$, and $0 < \lambda \leq 1$, on the unit circle for $z = e^{i\theta}$, $0 \leq \theta \leq 2\pi$. Figure 16 shows the locus of values of $f(z)$, where the unit circle is also drawn. As the figure and some algebra shows, only for $z = 1$, $\lambda = 0$, and $z = -1$, $\lambda = 1$, does $z = f(z)$.

Examining the first value $z = 1 = f(z)$, we have $\lambda = 0$, or equivalently $\Delta t = 0$, so $Q^{n+1} = Q^n$ (with $Q \in \{U, V, W\}$), which is clearly a stable solution. For the other case, we have $z = -1 = f(z)$, whose only solution (again using some numerical evaluation and some algebra) is $\lambda = 1$, $\alpha = 0$. But $\alpha = 0$ corresponds to the usual Lax–Wendroff scheme without the small cell, and $\lambda = 1$ for this case is straight copying of the solution ($\kappa = 0$, $\tau = -1$). Again this is stable.

Since Lax–Wendroff is a second order method, the use of linear interpolation with $O(h^2)$ error on a lower-dimensional set of points is reasonable. However, one might consider the use of quadratic interpolation for U_0, V_0 . The next question is what stencil to use for the quadratic interpolant. Using the notation of Figure 15, one might consider using the same interpolant based on V_{-1} , W , and U_1 to get both U_0 and V_0 . However, this choice reduces the stability region to $\lambda < .5$. If instead the interpolant for U_0 uses the surrounding points V_{-1} and W , and the third point is always the upwind point V_{-2} , full stability for a Courant number of $\lambda \leq 1$ is retained for all small cells with $0 < \alpha < 1$.

REFERENCES

- [1] M. J. BERGER, *Stability of interfaces with mesh refinement*, Math. Comp., 45 (1985), pp. 301–318.
- [2] M. J. BERGER, C. HELZEL, AND R. J. LEVEQUE, *H-Box Methods for the Approximation of Hyperbolic Conservation Laws on Irregular Grids*, Preprint 2002-022, Conservation law preprint server, <http://www.math.ntnu.no/conservation/2002/>.
- [3] M. J. BERGER AND R. J. LEVEQUE, *An adaptive Cartesian mesh algorithm for the Euler equations in arbitrary geometries*, in Proceedings of the 9th Computational Fluids Conference, AIAA paper AIAA-89-1930, Buffalo, NY, 1989, pp. 305–311.
- [4] M. J. BERGER AND R. J. LEVEQUE, *Cartesian meshes and adaptive mesh refinement for hyperbolic partial differential equations*, in Proceedings of the 3rd International Conference on Hyperbolic Problems, Uppsala, Sweden, 1990.

- [5] M. J. BERGER AND R. J. LEVEQUE, *Stable boundary conditions for Cartesian grid calculations*, *Comput. Syst. Engin.*, 1 (1990), pp. 305–311.
- [6] M. J. BERGER AND R. J. LEVEQUE, *A rotated difference scheme for Cartesian grids in complex geometries*, in *Proceedings of the 10th Computational Fluid Dynamics Conference*, AIAA paper CP-91-1602, Honolulu, Hawaii, 1991.
- [7] M. J. BERGER, R. J. LEVEQUE, AND L. G. STERN, *Finite volume methods for irregular one-dimensional grids*, in *Mathematics of Computation 1943–1993: A Half Century of Computational Mathematics*, *Proc. Sympos. Appl. Math.* 48, AMS, Providence, RI, 1994, pp. 255–259.
- [8] D. CALHOUN AND R. J. LEVEQUE, *A Cartesian grid finite-volume method for the advection diffusion equation in irregular geometries*, *J. Comput. Phys.*, 157 (2000), pp. 143–180.
- [9] J. FALCOVITZ, G. ALFANDARY, AND G. HANOCH, *A two-dimensional conservation laws scheme for compressible flows with moving boundaries*, *J. Comput. Phys.*, 138 (1997), pp. 83–102.
- [10] H. FORRER AND R. JELTSCH, *A high-order boundary treatment for Cartesian-grid methods*, *J. Comput. Phys.*, 140 (1998), pp. 259–277.
- [11] B. GUSTAFSSON, H.-O. KREISS, AND A. SUNDSTRÖM, *Stability theory of difference approximations for mixed initial boundary value problems. II*, *Math. Comp.*, 26 (1972), pp. 649–686.
- [12] H. O. KREISS, T. A. MANTEUFFEL, B. SWARTZ, B. WENDROFF, AND A. B. WHITE, *Supraconvergent schemes on irregular grids*, *Math. Comp.*, 47 (1986), pp. 537–554.
- [13] R. J. LEVEQUE, *CLAWPACK software*, <http://www.amath.washington.edu/~claw/>.
- [14] R. J. LEVEQUE, *Large time step shock-capturing techniques for scalar conservation laws*, *SIAM J. Numer. Anal.*, 19 (1982), pp. 1091–1109.
- [15] R. J. LEVEQUE, *Convergence of a large time step generalization of Godunov’s method for conservation laws*, *Comm. Pure Appl. Math.*, 37 (1984), pp. 463–477.
- [16] R. J. LEVEQUE, *A large time step generalization of Godunov’s method for systems of conservation laws*, *SIAM J. Numer. Anal.*, 22 (1985), pp. 1051–1073.
- [17] R. J. LEVEQUE, *High-resolution conservative algorithms for advection in incompressible flow*, *SIAM J. Numer. Anal.*, 33 (1996), pp. 627–665.
- [18] R. J. LEVEQUE, *Wave propagation algorithms for multidimensional hyperbolic systems*, *J. Comput. Phys.*, 131 (1997), pp. 327–353.
- [19] R. J. LEVEQUE, *Finite Volume Methods for Hyperbolic Problems*, Cambridge University Press, Cambridge, UK, 2002.
- [20] T. A. MANTEUFFEL AND A. B. WHITE, JR., *The numerical solution of second-order boundary value problems on nonuniform meshes*, *Math. Comp.*, 47 (1986), pp. 511–535.
- [21] D. MODIANO AND P. COLELLA, *A higher-order embedded boundary method for time dependent simulation of hyperbolic conservation laws*, in *Proceedings of the FEDSM 00 - ASME Fluids Engineering Simulation Meeting*, Boston, MA, 2000.
- [22] K. W. MORTON, *On the analysis of finite volume methods for evolutionary problems*, *SIAM J. Numer. Anal.*, 35 (1998), pp. 2195–2222.
- [23] R. B. PEMBER, J. B. BELL, P. COLELLA, W. Y. CRUTCHFIELD, AND M. L. WELCOME, *An adaptive Cartesian grid method for unsteady compressible flow in irregular regions*, *J. Comput. Phys.*, 120 (1995), pp. 278–304.
- [24] J. PIKE, *Grid adaptive algorithms for the solution of the Euler equations on irregular grids*, *J. Comput. Phys.*, 71 (1987), pp. 194–223.
- [25] J. J. QUIRK, *An alternative to unstructured grids for computing gas dynamic flows around arbitrarily complex two-dimensional bodies*, *Comput. & Fluids*, 23 (1994), pp. 125–142.
- [26] P. L. ROE, *Approximate Riemann solver, parameter vectors, and difference schemes*, *J. Comput. Phys.*, 43 (1981), pp. 357–372.
- [27] C. W. SCHULTZ-RINNE, J. P. COLLINS, AND H. M. GLAZ, *Numerical solution of the Riemann problem for two-dimensional gas dynamics*, *SIAM J. Sci. Comput.*, 14 (1993), pp. 1394–1414.
- [28] L. G. STERN, *An Explicit Conservative Method for Time-Accurate Solution of Hyperbolic Partial Differential Equations on Embedded Chimera Grids*, Ph.D. thesis, University of Washington, Seattle, WA, 1996. Available from <ftp://www.amath.washington.edu/pub/~rjl/students/stern:thesis.ps.gz>.
- [29] B. VAN LEER, *Towards the ultimate conservative difference scheme II. Monotonicity and conservation combined in a second order scheme*, *J. Comput. Phys.*, 14 (1974), pp. 361–370.
- [30] B. WENDROFF AND A. B. WHITE, *Some supraconvergent schemes for hyperbolic equations on nonuniform grids*, in *Proceedings of the Second International Conference on Hyperbolic Problems*, Aachen, Germany, 1988, pp. 671–677.
- [31] B. WENDROFF AND A. B. WHITE, *A supraconvergent scheme for nonlinear hyperbolic systems*, *Comput. Math. Appl.*, 18 (1989), pp. 761–767.